

Gaussian curvature and Lyapunov exponent as probes of black hole phase transitions

Shi-Hao Zhang,¹ Zi-Qiang Zhao,¹ Zi-Yuan Li,² Jing-Fei Zhang,^{1,*} and Xin Zhang^{1,3,4,†}

¹*Key Laboratory of Cosmology and Astrophysics (Liaoning),
College of Sciences, Northeastern University, Shenyang 110819, China*

²*School of Physics, Nankai University, Tianjin 300071, China*

³*Key Laboratory of Data Analytics and Optimization for Smart Industry (Ministry of Education),
Northeastern University, Shenyang 110819, China*

⁴*National Frontiers Science Center for Industrial Intelligence and Systems Optimization,
Northeastern University, Shenyang 110819, China*

First-order phase transitions of black holes have been extensively studied within thermodynamic frameworks, yet the corresponding evolution of spacetime geometric properties remains unclear. This paper establishes a purely differential geometric framework to probe such phase transitions by analyzing the curvature of unstable null orbits. Using the geodesic curvature of the optical metric to locate the light ring, we demonstrate that the corresponding Gaussian curvature K serves as a direct geometric signature of the phase transition. During a first-order phase transition, the curve K versus temperature T exhibits a multivalued structure within the spinodal region, precisely mirroring the swallowtail behavior of the free energy. Numerical analysis of Hayward-Letelier-AdS black holes confirms the effectiveness of this geometric signature. Our work demonstrates that the intrinsic geometric quantities of spacetime encode the information of black hole phase transitions. These quantities serve simultaneously as geometric probes and order parameters for black hole phase transitions. This result provides a purely geometric foundation for understanding the correspondence between thermodynamics and spacetime curvature in the null case.

I. INTRODUCTION

Since the 1970s studies by Bekenstein and Hawking [1, 2], black holes have been regarded as thermodynamic systems. Subsequent studies revealed that black holes can undergo phase transitions, such as the Hawking-Page phase transition [3]. Later studies showed that when the cosmological constant is treated as pressure, black holes exhibit a van der Waals-like first-order phase transition [4] and a reentrant phase transition [5]. Furthermore, building on the holographic principle in black hole thermodynamics, Maldacena established the AdS/CFT correspondence [6] in 1997. Further investigation within this duality showed that black holes as quantum thermodynamic systems exhibit chaos and that their Lyapunov exponents obey the MSS bound $\lambda \leq 2\pi T/\hbar$ [7–9]. In recent years, some studies have applied classical dynamics methods to verify the validity of the MSS bound [10–14]. The Lyapunov exponent not only directly characterizes the chaotic behavior of black holes as quantum thermodynamic systems, but has also been connected to the imaginary part of quasinormal modes (QNMs) [15, 16].

In black hole thermodynamics, the multivaluedness of QNMs [17–26] and Lyapunov exponents [27–37] during first-order phase transitions suggest a potential connection between these quantities and black hole phase transitions. Studies of the observable photon sphere have also tied it to black hole phase transitions [38–46], confirming that dynamical analysis can probe such phenomena. However, one question remains largely unexplored. Since

general relativity is fundamentally geometric, how does spacetime geometry itself change during a thermal phase transition? Is there an intrinsic geometric quantity that can directly reflect this phase transition?

Black holes are exact solutions of the Einstein equations whose physical processes are reflected by changes in geometric properties. Gaussian curvature, an intrinsic measure of a two-dimensional manifold, directly quantifies local spacetime curvature and serves as an ideal probe of geometry. Using Gaussian curvature, researchers have developed purely geometric methods to study black hole photon spheres [47, 48], thus establishing a clear correspondence between dynamics and geometry. Recently, it has been used to analyze the stability of circular orbits for massless particles, to determine the existence and distribution of stable and unstable orbits [49], and to investigate gravitational lensing by massive particles [50, 51]. This raises a previously overlooked question: can geometric quantities such as Gaussian curvature be used to connect with first-order phase transitions of a black hole? A key finding is that the Lyapunov exponent of null circular orbits near black holes is linked to their Gaussian curvature [52]. The established role of the Lyapunov exponent as an effective probe makes it possible to address the above question.

In this work, we investigate unstable particle orbits near a 3+1-dimensional spherically symmetric black hole. We demonstrate that the Gaussian curvature of unstable orbits of massless particles is multivalued at black hole phase transition point, offering a new perspective for understanding black hole phase transitions. This reveals that during such phase transitions, characterized by the existence of multiple spacetime solutions, the corresponding geometric quantity exhibits multivalued behavior.

* jfzhang@neu.edu.cn

† zhangxin@neu.edu.cn

This paper is arranged as follows. In Sec. II, we briefly review the relations of black hole thermodynamics, the Gaussian curvature of two-dimensional surfaces, and the calculation of Lyapunov exponents. In Sect. III, we present the investigation of the Hayward-Letelier-AdS black hole and the analysis of the results. In Sec. IV, we address the computation of critical exponents. In Sec. V, we offer a summary and discussion, and the appendix follows. We set $G = c = k_B = \hbar = 1$ in this paper.

II. THEORETICAL FRAMEWORK

In this section, we first briefly review the relations of black hole thermodynamics, then introduce how to obtain the Gaussian curvature from a two-dimensional Riemannian metric, and finally recall the derivation of the Lyapunov exponent and its connection to the Gaussian curvature.

A. Thermodynamics and phase structure of spherically symmetric black holes

In this subsection, we briefly review the relations in black hole thermodynamics by considering a 3+1-dimensional spherically symmetric black hole solution

$$ds^2 = -f(r)dt^2 + \frac{1}{f(r)}dr^2 + r^2(d\theta^2 + \sin^2\theta d\phi^2). \quad (1)$$

Note that $f(r_+) = 0$, where r_+ is the horizon radius. The temperature can be obtained directly from the first law of a charged and static black hole in extended phase space as [53]

$$T = \frac{\partial M}{\partial S}, \quad (2)$$

for a fixed charge and pressure. The Gibbs free energy is

$$F = M - TS, \quad (3)$$

where $S = A/4 = \pi r_+^2$ is the entropy, A is the area of the black hole horizon. If a first-order phase transition occurs, the free energy exhibits a swallowtail structure, indicating the appearance of three black hole solutions (large black hole, intermediate black hole, and small black hole). The critical point is determined by the following condition

$$\frac{\partial T}{\partial r_+} = \frac{\partial^2 T}{\partial r_+^2} = 0. \quad (4)$$

For an Anti-de Sitter spacetime, the pressure is given by [4]:

$$P = -\frac{\Lambda}{8\pi} = \frac{3}{8\pi\ell^2}, \quad (5)$$

where Λ is a cosmological constant and ℓ is the AdS radius.

B. Gaussian curvature of two-dimensional manifolds

Gaussian curvature K is an intrinsic geometric quantity of the optical metric associated with massless particles, and the light ring is closely linked to black hole spacetime. This suggests that K on the light ring may exhibit anomalous behavior near the phase transition point, offering a potential geometric signature for studying such phase transitions.

Consider a static 3+1-dimensional spherically symmetric metric

$$ds^2 = -f(r)dt^2 + \frac{1}{g(r)}dr^2 + r^2d\Omega^2, \quad (6)$$

where $d\Omega^2$ is the unit 2-sphere, and $f(r)$ and $g(r)$ are smooth functions of class C^P ($P \geq 2$).

To analyze null geodesics, we rewrite Eq. (6) as the optical metric ($ds^2 = 0$), and restrict our attention to the metric in the equatorial plane ($\theta = \frac{\pi}{2}$)

$$dt^2 = \frac{1}{f(r)} \left(\frac{1}{g(r)}dr^2 + r^2d\phi^2 \right). \quad (7)$$

Beginning with Eq. (7), which describes a two-dimensional Riemannian manifold, we compute the Gaussian curvature associated with distinct null circular orbits. For a two-dimensional Riemannian manifold in orthogonal coordinates, its Gaussian curvature is given by

$$K = -\frac{1}{2\sqrt{EG}} \left\{ \frac{\partial}{\partial v} \left[\frac{(E)_v}{\sqrt{EG}} \right] + \frac{\partial}{\partial u} \left[\frac{(G)_u}{\sqrt{EG}} \right] \right\}, \quad (8)$$

where (u, v) are the coordinate variables on the surface, and E, G are the coefficients of the first fundamental form [48]. By setting $E = g_{11}$ and $G = g_{22}$, Eq. (8) translates Gaussian notation into tensor notation

$$K = -\frac{1}{2} \frac{1}{\sqrt{g_{rr}g_{\phi\phi}}} \frac{d}{dr} \left(\frac{g'_{\phi\phi}}{\sqrt{g_{rr}g_{\phi\phi}}} \right). \quad (9)$$

Substituting Eq. (7) into (9) yields

$$K(r) = -g'(r) \frac{2f(r) - rf'(r)}{4r} + \frac{g(r)}{2} \left[f'(r) \left(\frac{1}{r} - \frac{f'(r)}{f(r)} \right) + f''(r) \right]. \quad (10)$$

Consider the optical metric given in Eq. (7), its geodesic curvature κ_g is given by

$$\kappa_g = \sqrt{\frac{g(r)}{f(r)}} \frac{2f(r) - rf'(r)}{2r}. \quad (11)$$

On the unstable null circular orbit $r = r_{LR}$ (the light ring), the geodesic curvature vanishes, yielding

$$2f(r_{LR}) = r_{LR}f'(r_{LR}). \quad (12)$$

For the unstable null circular orbit ($r = r_{LR}$, inserting Eq. (12) into (10) yields a known relation [52]

$$K(r_{LR}) = \left\{ \frac{g(r)}{2} \left[f''(r) - \frac{f'(r)}{r} \right] \right\} \Big|_{r=r_{LR}}. \quad (13)$$

Note that $K(r_{LR})$ depends only on the derivatives of the spherically symmetric black hole metric functions $g(r)$ and $f(r)$. As an intrinsic geometric quantity of a surface, the Gaussian curvature depends solely on the first fundamental form of the surface (a profound result known as the *Egregium Theorem*). It quantifies the deviation of the first fundamental form of the two-dimensional surface from the Euclidean metric, which is fundamental to the study of intrinsic geometry [48]. As a coordinate-invariant intrinsic curvature, K directly measures space-time deformation, unlike orbital stability analyses.

In Sec. III, we will demonstrate the connection between Gaussian curvature and first-order phase transitions by examining the anomalous behavior of K for circular null orbits near the Hayward-Letelier-AdS. A more explicit link between the detailed behavior of K and the phase transition will be provided in the next subsection through the analysis of Lyapunov exponents.

C. Lyapunov exponent for unstable orbits

The Lyapunov exponent λ is a dynamical quantity that characterizes the chaotic behavior of particle orbits near black holes, and it does not directly reflect a phase transition. In this subsection, we briefly review the derivation of λ and its relationship with K .

Beginning with the metric Eq. (6), the Lagrangian is

$$\mathcal{L} = g_{\mu\nu} \dot{x}^\mu \dot{x}^\nu = \sigma, \quad (14)$$

where $\sigma = \{+1, -1, 0\}$ denotes spacelike, timelike, and null geodesics, respectively. The angular momentum and energy are defined by

$$2L = 2 \frac{\partial \mathcal{L}}{\partial \dot{\phi}} = 2r^2 \dot{\phi}, \quad -2E = 2 \frac{\partial \mathcal{L}}{\partial \dot{t}} = -2f\dot{t}. \quad (15)$$

On the equatorial plane, the radial motion follows

$$(\dot{r})^2 = V_{\text{eff}}(r), \quad (16)$$

with effective potential

$$V_{\text{eff}}(r) = g(r) \left[\frac{E^2}{f(r)} - \frac{L^2}{r^2} - \sigma \right]. \quad (17)$$

For massless particles $\sigma = 0$, the second derivative on light rings r_{LR} satisfies

$$V''_{\text{eff}}(r_{LR}) = \frac{g(r)L^2}{r^4 f(r)} \left[r f'(r) - r^2 f''(r) \right] \Big|_{r=r_{LR}}. \quad (18)$$

Expanding this equation of motion at the light ring yields

$$(\dot{\varepsilon})^2 - \frac{1}{2} V''_{\text{eff}}(r_{LR}) \varepsilon^2 = 0, \quad (19)$$

where $\varepsilon = r - r_{LR}$. Note that this is an inverted harmonic oscillator equation, defining the Lyapunov exponent [15, 54]

$$\lambda = \sqrt{\frac{1}{2(\dot{t})^2} V''_{\text{eff}}(r_{LR})}. \quad (20)$$

The general solution is

$$\varepsilon = A e^{\lambda t} + B e^{-\lambda t}. \quad (21)$$

Combining Eqs. (15), (20), and (13) yields a known relation [52]

$$K(r_{LR}) = -\lambda^2(r_{LR}). \quad (22)$$

Eq. (22) establishes a quantitative relation between Gaussian curvature and Lyapunov exponent on the light ring. Previous studies [27–29, 31–36] have demonstrated that λ becomes multivalued near the phase transition point. In Refs. [27, 32], the authors interpreted the Lyapunov exponent as an order parameter that decreases with increasing temperature T . Clearly, Eq. (22) provides a mapping between K and λ on the light ring. Such a mapping paves the way for a connection between geometry and thermodynamics, thereby enabling the investigation of thermodynamics from a geometric perspective. Combined with Eq. (22), if λ is multivalued in the spinodal region, K must also be multivalued, offering a geometric way to probe black hole phase transitions. Note that not only do null circular orbits admit a Lyapunov exponent, but circular orbits of massive particles can also be defined. In both cases, these dynamical quantities connect with the phase transition.

For completeness, we also examine the Lyapunov exponent associated with the circular orbits of massive particles. The corresponding unstable circular orbit is located at $r = r_0$ with $\sigma = -1$, and its Lyapunov exponent is given by

$$\begin{aligned} \lambda &= \frac{1}{2} \sqrt{[2f(r) - r f'(r)] V''_{\text{eff}}(r)} \Big|_{r=r_0} \\ &= \frac{1}{\sqrt{2}} \sqrt{-\frac{g(r_0)}{f(r_0)} \left[\frac{3f(r_0)f'(r_0)}{r_0} - 2f'(r_0)^2 + f(r_0)f''(r_0) \right]}. \end{aligned} \quad (23)$$

For $g(r) = f(r)$, the conserved quantities satisfy

$$\frac{E}{L} = \frac{\sqrt{f(r_0)}}{r_0}. \quad (24)$$

In Sec. III, we also examine the relationship between λ and \tilde{T} , where the tilde denotes dimensionless quantities, for massless and massive particles around a specific black hole.

III. NUMERICAL RESULTS AND ANALYSIS

In Sec. II, we established a theoretical framework valid for static 3+1-dimensional spherically symmetric black holes. This section will probe the Hayward-Letelier-AdS black hole, and we will examine our conjecture by following these steps. We first examine the $\tilde{F}(\tilde{T})$ curve to determine the spinodal region $(\tilde{T}_1, \tilde{T}_2)$ from its characteristic multivaluedness. We then investigate whether the corresponding $K(\tilde{T})$ and $\lambda(\tilde{T})$ curves also become multivalued within the same temperature interval.

We investigate the behavior of $\lambda(\tilde{T})$ and $K(\tilde{T})$ for null geodesics near the phase transition point \tilde{T}_p in the Hayward-Letelier-AdS black hole. This solution corresponds to a Hayward black hole in AdS spacetime surrounded by a cloud of strings [53]. Its metric function is

$$f_{HL}(r) = 1 - \frac{2Mr^2}{g^3 + r^3} + \frac{r^2}{\ell^2} - a, \quad (25)$$

where g is the magnetic monopole charge, ℓ is the AdS radius, and the string-cloud parameter a arises from the string-cloud term in action [53]. For studies of Hayward-AdS black holes with string fluids in the extended thermodynamic phase space, see Ref. [55] for thermodynamic curvature and topological properties, and Ref. [56] for chaotic behavior. When $a = 0$, the metric reduces to the Hayward-AdS black hole. The temperature is [55]

$$T_{HL} = \frac{r_+^3 [(1-a) + 3r_+^2/\ell^2] - 2g^3(1-a)}{4\pi r_+^4}. \quad (26)$$

The Gibbs free energy is

$$F_{HL} = \frac{1}{4} \left\{ g^3 \left[\frac{2}{\ell^2} + \frac{4(1-a)}{r_+^2} \right] + (1-a)r_+ - \frac{r_+^3}{\ell^2} \right\}. \quad (27)$$

Here,

$$M = \left(1 + \frac{r_+^2}{\ell^2} - a \right) \frac{g^3 + r_+^3}{2r_+^2}. \quad (28)$$

Since a is a dimensionless constant, We introduce the following scaling

$$\tilde{r}_+ = \frac{r_+}{\ell}, \quad \tilde{g} = \frac{g}{\ell}, \quad \tilde{M} = \frac{M}{\ell}, \quad \tilde{F}_H = \frac{F_H}{\ell}, \quad \tilde{T}_H = T_H \ell. \quad (29)$$

We present the $\tilde{F}_{HL}(\tilde{T}_{HL})$, $K_{HL}(\tilde{T}_{HL})$, and $\lambda_{HL}(\tilde{T}_{HL})$ curves for the Hayward-Letelier-AdS black hole.

As illustrated in Fig. 1(a), for $\tilde{g} < \tilde{g}_c$ the swallowtail structure indicates a first-order phase transition. Similarly, in Figs. 1(b), 1(c), and 1(d), the $K_{HL}(\tilde{T}_{HL})$ curve for null circular orbits and the $\lambda_{HL}(\tilde{T}_{HL})$ curve for both timelike and null orbits exhibit multivalued behavior. This shows that both the Gaussian curvature K_{HL} and the Lyapunov exponent λ_{HL} are intimately related to the

first-order phase transition, because Eq. (22) connects chaotic dynamics and geometry. This connection paves the way for studying thermodynamics from a geometric perspective.

Moreover, we find that the Gaussian curvature K_{HL} of the unstable null circular orbits in Fig. 1(b) is consistently negative, in full agreement with the result of Ref. [47]. In Ref. [47], the authors adopted an alternative approach based on the Hadamard theorem, demonstrating that $K < 0$ corresponds to unstable circular orbits, while $K > 0$ indicates stable ones. Our results show that the Gaussian curvature on the light ring is strictly negative, supporting their conclusion. Additionally, after the black hole undergoes a first-order phase transition, specifically on the right side of the spinodal region, $|K|$ decreases monotonically with increasing temperature \tilde{T} . This behavior suggests that K may be related to the order parameter, a finding consistent with other recent studies Refs. [27, 32, 57, 58]. These results indicate that the Gaussian curvature becomes multivalued whenever the black hole experiences a phase transition.

In contrast, as illustrated in Fig. 2(a), for the case $\tilde{g} > \tilde{g}_c$ where no first-order phase transition occurs, Fig. 2(b) shows that $K_{HL}(\tilde{T}_{HL})$ becomes a monotonic function of \tilde{T}_{HL} . Thus, the multivalued behavior of K and λ serves as a robust geometric characterization of the first-order phase transition phenomenon and its associated spinodal region, revealing a profound link between spacetime geometry and thermodynamics.

IV. CRITICAL EXPONENT FROM LYAPUNOV EXPONENTS AND GAUSSIAN CURVATURE

Critical exponents are used to describe the behavior of physical quantities of thermodynamic systems near the critical point and serve as important physical quantities for characterizing phase transitions. At the phase transition point, the small and large black hole branches coexist, leading to discontinuities in both the null Lyapunov exponent and the Gaussian curvature. This section will examine the continuity of the null Lyapunov exponent and Gaussian curvature for the Hayward-Letelier-AdS black hole at the phase transition point T_p , as well as their discontinuity near T_p , investigating whether they can serve as order parameters and calculating their critical exponents.

We define the null Lyapunov exponents for the small and large black hole branches within the spinodal region as λ_S and λ_L , respectively, and the corresponding Gaussian curvatures as K_S and K_L . Their differences are defined as $\Delta\lambda$ and ΔK . When the critical point $T_p = T_c$, we have $\Delta\lambda = \Delta K = 0$. We will fit the numerical coefficients of $\Delta\lambda$ and ΔK according to the following form [38]

$$\frac{\Delta\lambda}{\lambda_c}, \frac{\Delta K}{K_c} \sim \alpha(t-1)^\beta. \quad (30)$$

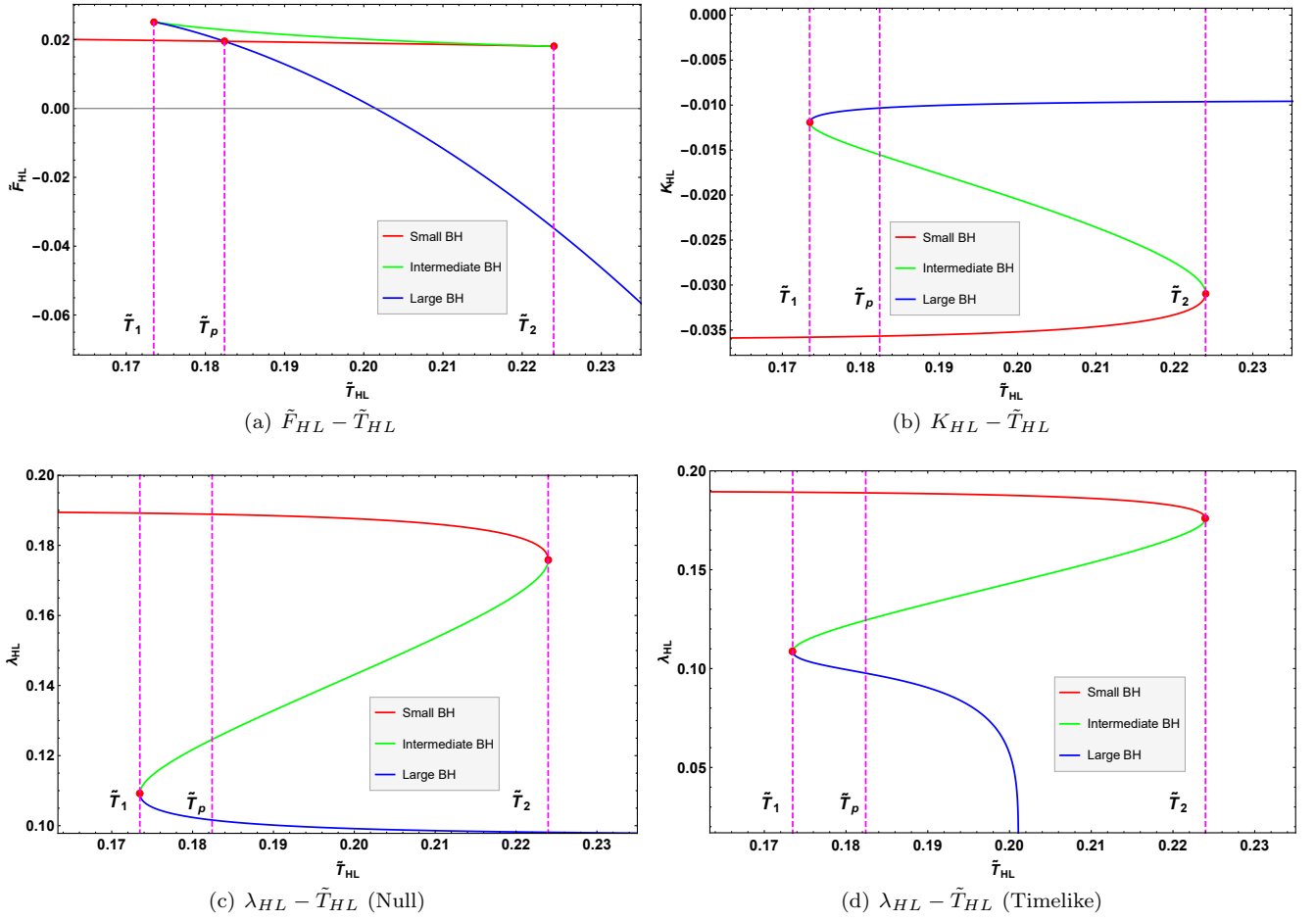


FIG. 1. Thermodynamic, geometric and chaos signatures of the first-order phase transition in Hayward-Letelier-AdS spacetimes. (a) \tilde{F}_{HL} , (b) K_{HL} of unstable null orbits and (c-d) λ_{HL} of unstable null/timelike orbits versus temperature \tilde{T}_{HL} for Hayward-Letelier-AdS black holes, and $\tilde{g} = 0.0615$, $\tilde{g}_c = 0.1042$, $a = 0.6$, $\tilde{g} < \tilde{g}_c$, $L = 20\ell$. Swallowtail structures in \tilde{F}_{HL} and multivalued K_{HL} at \tilde{T}_p evidence geometric degeneracy during phase transitions. λ_{HL} at \tilde{T}_p also exhibits such multivaluedness.

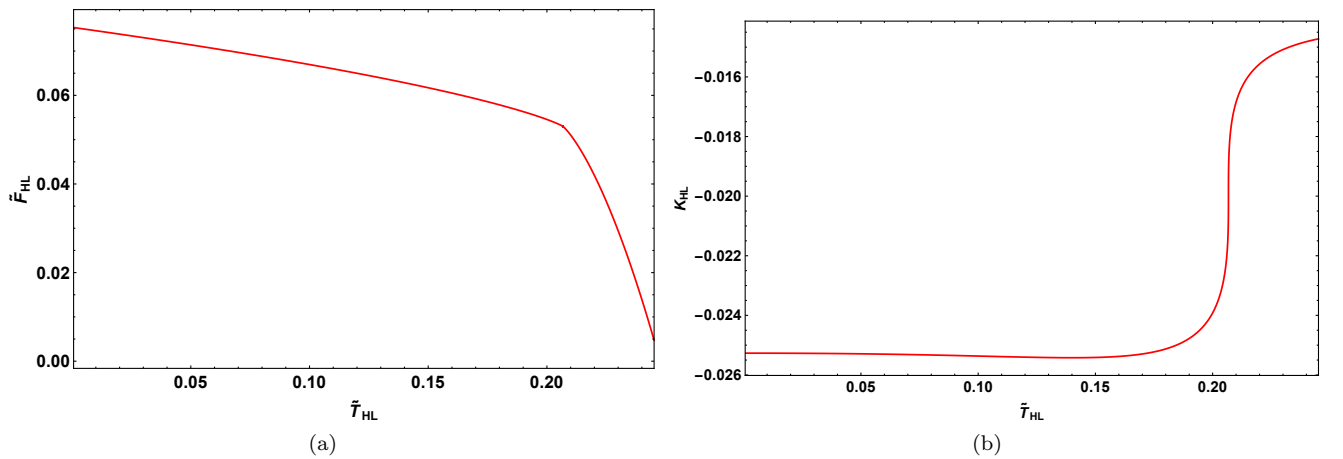


FIG. 2. Thermodynamic and geometric signatures of the absence of a first-order phase transition in Hayward-Letelier-AdS spacetimes. (a) Free energy \tilde{F}_{HL} and (b) Gaussian curvature K_{HL} versus temperature \tilde{T}_{HL} for a Hayward-Letelier-AdS black hole without phase transition ($\tilde{g} = 0.0615$, $\tilde{g}_c = 0.1042$, $a = 0.6$, $\tilde{g} > \tilde{g}_c$). Both quantities exhibit monotonic behavior, confirming the absence of thermodynamic criticality.

Here, $t = T_p/T_c$, α and β are real numbers, the subscript “ c ” denotes the value of the Lyapunov exponent and Gaussian curvature at the critical point.

As shown in Fig. 3, we plot the normalized differences $\Delta\lambda/\lambda_c$ and $\Delta K/K_c$ as functions of the reduced temperature t . When $T_p = T_c$, $\Delta\lambda/\lambda_c = \Delta K/K_c = 0$. When T_p deviates from T_c , both $\Delta\lambda/\lambda_c$ and $\Delta K/K_c$ take non-zero values, indicating the emergence of discontinuity. Ultimately, we obtain the following analytical expressions

$$\frac{\Delta\lambda}{\lambda_c} \simeq 6.9374(t-1)^{0.5761}, \quad (31)$$

and

$$\frac{\Delta K}{K_c} \simeq 49.5398(t-1)^{0.6032}. \quad (32)$$

These results indicate that $\Delta\lambda/\lambda_c$ and $\Delta K/K_c$ can serve as order parameters. However, their critical exponents deviate from the exponent of 1/2 observed in Reissner-Nordström black holes, suggesting that the geometry and dynamics of regular black holes exhibit richer critical behavior compared to singular black holes.

V. DISCUSSION

In this work, we systematically investigate the profound connections between spacetime geometry, thermodynamics, and chaos dynamics during first-order phase transitions of black holes. While the standard thermodynamic methods describe phase transitions through the behavior of thermodynamic potentials, the corresponding evolution of spacetime geometry itself demands a more direct description. Based on this consideration, we examine the possibility of employing the intrinsic geometric quantity Gaussian curvature K as a new probe.

We find that during a first-order phase transition, the Gaussian curvature of unstable null orbits exhibits multivalued behavior inside the spinodal region and coincides precisely with the swallowtail structure of the free energy. This phenomenon can be understood through the known relation $K(r_{LR}) = -\lambda^2(r_{LR})$, whereby the Gaussian curvature inherits the multivalued nature of the Lyapunov exponent. However, this relation should not be interpreted as a mere translation of the dynamical results into geometric language. The key advance of our work lies in establishing a self-contained geometric diagnostic framework that operates independently of

any dynamical calculation. The procedure is purely geometric: first, determining the light ring radius from the geodesic curvature of the optical metric, then computing the corresponding Gaussian curvature via the first fundamental form, and finally, checking for multivalued behavior. This self-consistent procedure yields results in precise agreement with thermodynamic predictions.

Through numerical analysis of the Hayward-Letelier-AdS black hole, we find that when the parameter \tilde{g} enters the spinodal region, the free energy exhibits a swallowtail structure, while both the Gaussian curvature K and the Lyapunov exponent λ exhibit multivalued behavior. The temperature intervals over which this occurs align precisely with the thermodynamic spinodal region. Furthermore, we demonstrate that in the absence of a phase transition ($\tilde{g} > \tilde{g}_c$), the Gaussian curvature K varies monotonically and the geometric multivaluedness disappears. This confirms that the multivalued behavior of the Gaussian curvature is a geometric signature of the phase transition.

Near the critical point, the scaling laws of the Gaussian curvature and the null Lyapunov exponent for the Hayward-Letelier-AdS black hole deviate from those observed in most black hole solutions, suggesting that regular black holes may exhibit more interesting dynamical and geometric behaviors.

These results advance the paradigm from standard thermodynamic or dynamical frameworks toward a purely geometric perspective. They indicate that black hole first-order phase transitions can be fundamentally understood as a branching behavior in the curvature structure of spacetime. Our work provides the direct evidence of the accompanying degeneracy in spacetime geometry during such phase transitions and demonstrates that Gaussian curvature can serve as a self-consistent diagnostic probe. This opens a new pathway for studying black hole phase structures from a geometric perspective.

VI. ACKNOWLEDGEMENTS

This work was supported by the National Natural Science Foundation of China (Grants Nos. 12473001, 12575049, and 12533001), the National SKA Program of China (Grants Nos. 2022SKA0110200 and 2022SKA0110203), the China Manned Space Program (Grant No. CMS-CSST-2025-A02), and the 111 Project (Grant No. B16009).

-
- [1] S. W. Hawking, *Commun. Math. Phys.* **43**, 199 (1975), [Erratum: *Commun.Math.Phys.* 46, 206 (1976)].
 [2] J. D. Bekenstein, *Phys. Rev. D* **7**, 2333 (1973).
 [3] S. W. Hawking and D. N. Page, *Commun. Math. Phys.* **87**, 577 (1983).

- [4] D. Kubiznak and R. B. Mann, *JHEP* **07**, 033 (2012), [arXiv:1205.0559 \[hep-th\]](#).
 [5] N. Altamirano, D. Kubiznak, and R. B. Mann, *Phys. Rev. D* **88**, 101502 (2013), [arXiv:1306.5756 \[hep-th\]](#).
 [6] J. M. Maldacena, *Adv. Theor. Math. Phys.* **2**, 231 (1998), [arXiv:hep-th/9711200](#).

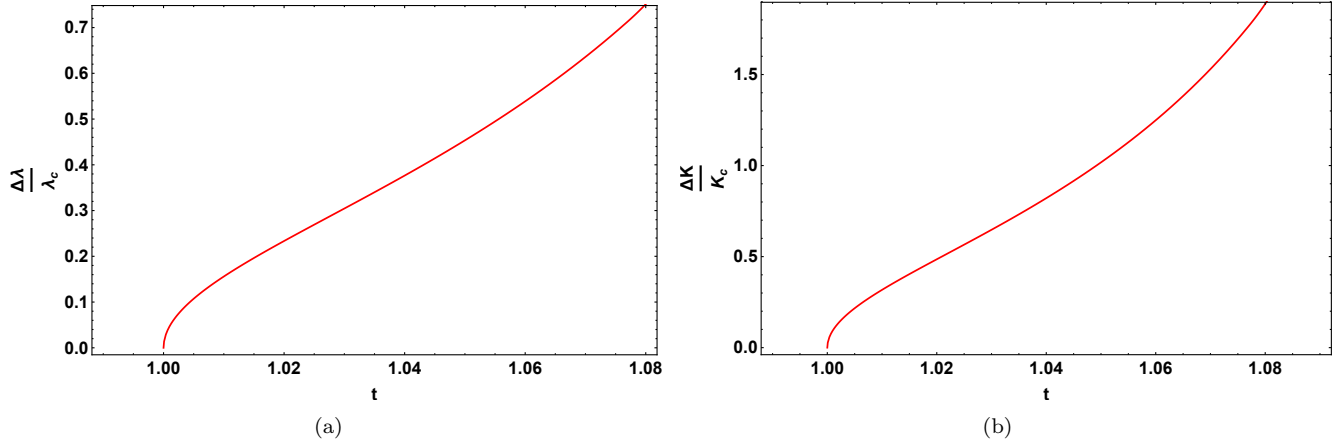


FIG. 3. The reduced null Lyapunov exponents and Gaussian curvatures for the coexistence small and large black holes. (a) Null Lyapunov exponents and (b) Gaussian curvature K_{HL} versus reduced temperature t for a Hayward-Letelier-AdS black hole.

- [7] S. H. Shenker and D. Stanford, *JHEP* **3**, 67 (2014), [arXiv:1306.0622 \[hep-th\]](#).
- [8] S. H. Shenker and D. Stanford, *JHEP* **3**, 46 (2014), [arXiv:1312.3296 \[hep-th\]](#).
- [9] J. Maldacena, S. H. Shenker, and D. Stanford, *JHEP* **08**, 106 (2016), [arXiv:1503.01409 \[hep-th\]](#).
- [10] K. Hashimoto and N. Tanahashi, *Phys. Rev. D* **95**, 024007 (2017).
- [11] Q.-Q. Zhao, Y.-Z. Li, and H. Lü, *Phys. Rev. D* **98**, 124001 (2018).
- [12] S. Dalui, B. R. Majhi, and P. Mishra, *Phys. Lett. B* **788**, 486 (2019), [arXiv:1803.06527 \[gr-qc\]](#).
- [13] Y.-Q. Lei, X.-H. Ge, and C. Ran, *Phys. Rev. D* **104**, 046020 (2021).
- [14] N. Kan and B. Gwak, *Phys. Rev. D* **105**, 026006 (2022).
- [15] V. Cardoso, A. S. Miranda, E. Berti, H. Witek, and V. T. Zanchin, *Phys. Rev. D* **79**, 064016 (2009).
- [16] G. Guo, P. Wang, H. Wu, and H. Yang, *JHEP* **06**, 060 (2022), [arXiv:2112.14133 \[gr-qc\]](#).
- [17] Y. Liu, D.-C. Zou, and B. Wang, *JHEP* **09**, 179 (2014), [arXiv:1405.2644 \[hep-th\]](#).
- [18] S. Mahapatra, *JHEP* **04**, 142 (2016), [arXiv:1602.03007 \[hep-th\]](#).
- [19] M. Chabab, H. El Moumni, S. Iraoui, and K. Masmar, *Eur. Phys. J. C* **76**, 676 (2016), [arXiv:1606.08524 \[hep-th\]](#).
- [20] D.-C. Zou, Y. Liu, and R.-H. Yue, *Eur. Phys. J. C* **77**, 365 (2017), [arXiv:1702.08118 \[gr-qc\]](#).
- [21] M. Zhang, C.-M. Zhang, D.-C. Zou, and R.-H. Yue, *Chin. Phys. C* **45**, 045105 (2021), [arXiv:2009.03096 \[hep-th\]](#).
- [22] Z.-Q. Zhao, X.-K. Zhang, and Z.-Y. Nie, *JHEP* **02**, 023 (2023), [arXiv:2211.14762 \[hep-th\]](#).
- [23] X. Zhao, Z.-Y. Nie, Z.-Q. Zhao, H.-B. Zeng, Y. Tian, and M. Baggioli, *JHEP* **02**, 184 (2024), [arXiv:2311.08277 \[hep-th\]](#).
- [24] Z.-Q. Zhao, Z.-Y. Nie, J.-F. Zhang, X. Zhang, and M. Baggioli, *Eur. Phys. J. C* **85**, 464 (2025), [arXiv:2406.05345 \[hep-th\]](#).
- [25] Z.-Q. Zhao, Z.-Y. Nie, J.-F. Zhang, and X. Zhang, (2025), [arXiv:2504.04995 \[gr-qc\]](#).
- [26] Z.-Y. Hou, Y.-Q. Lei, and X.-H. Ge, (2025), [arXiv:2508.00404 \[hep-th\]](#).
- [27] X. Guo, Y. Lu, B. Mu, and P. Wang, *JHEP* **08**, 153 (2022), [arXiv:2205.02122 \[gr-qc\]](#).
- [28] S. Yang, J. Tao, B. Mu, and A. He, *Journal of Cosmology and Astroparticle Physics* **2023**, 045 (2023).
- [29] X. Lyu, J. Tao, and P. Wang, *Eur. Phys. J. C* **84**, 974 (2024), [arXiv:2312.11912 \[gr-qc\]](#).
- [30] A. N. Kumara, S. Punacha, and M. S. Ali, *JCAP* **07**, 061 (2024), [arXiv:2401.05181 \[gr-qc\]](#).
- [31] Y.-Z. Du, H.-F. Li, Y.-B. Ma, and Q. Gu, *Eur. Phys. J. C* **85**, 78 (2025), [arXiv:2403.20083 \[hep-th\]](#).
- [32] B. Shukla, P. P. Das, D. Dudal, and S. Mahapatra, *Phys. Rev. D* **110**, 024068 (2024).
- [33] N. J. Gogoi, S. Acharjee, and P. Phukon, *Eur. Phys. J. C* **84**, 1144 (2024), [arXiv:2404.03947 \[hep-th\]](#).
- [34] D. Chen, C. Yang, and Y. Liu, *Physics Letters B* **865**, 139463 (2025).
- [35] K. M. A. Karthik R., Dillirajan D. and K. Hegde, arXiv preprint [arXiv:2504.12890](#) (2025).
- [36] M. B. Awal and P. Phukon, arXiv preprint [arXiv:2505.20800](#) (2025).
- [37] C. Yang, C. Gao, D. Chen, and X. Zeng, (2025), [arXiv:2506.21882 \[hep-th\]](#).
- [38] S.-W. Wei and Y.-X. Liu, *Phys. Rev. D* **97**, 104027 (2018).
- [39] S.-W. Wei, Y.-X. Liu, and Y.-Q. Wang, *Phys. Rev. D* **99**, 044013 (2019), [arXiv:1807.03455 \[gr-qc\]](#).
- [40] M. Zhang, S.-Z. Han, J. Jiang, and W.-B. Liu, *Phys. Rev. D* **99**, 065016 (2019), [arXiv:1903.08293 \[hep-th\]](#).
- [41] Y.-M. Xu, H.-M. Wang, Y.-X. Liu, and S.-W. Wei, *Phys. Rev. D* **100**, 104044 (2019), [arXiv:1906.03334 \[gr-qc\]](#).
- [42] H. Li, Y. Chen, and S.-J. Zhang, *Nucl. Phys. B* **954**, 114975 (2020), [arXiv:1908.09570 \[hep-th\]](#).
- [43] A. Naveena Kumara, C. L. Ahmed Rizwan, S. Punacha, K. M. Ajith, and M. S. Ali, *Phys. Rev. D* **102**, 084059 (2020), [arXiv:1912.11909 \[gr-qc\]](#).

- [44] Y.-Z. Du, H.-F. Li, F. Liu, and L.-C. Zhang, *JHEP* **01**, 137 (2023), [arXiv:2204.01007 \[hep-th\]](#).
- [45] A. Kumar, S. G. Ghosh, and A. Wang, *Phys. Dark Univ.* **46**, 101608 (2024).
- [46] S.-J. Yang, S.-P. Wu, S.-W. Wei, and Y.-X. Liu, arXiv preprint [arXiv:2505.20860](#) (2025), [arXiv:2505.20860 \[gr-qc\]](#).
- [47] C.-K. Qiao and M. Li, *Phys. Rev. D* **106**, L021501 (2022), [arXiv:2204.07297 \[gr-qc\]](#).
- [48] W.-H. Chern, *Differential Geometry* (Peking University Press, 2006).
- [49] C.-K. Qiao, *Eur. Phys. J. C* **85**, 191 (2025), [arXiv:2407.14035 \[gr-qc\]](#).
- [50] Z. Li, G. Zhang, and A. Övgün, *Phys. Rev. D* **101**, 124058 (2020), [arXiv:2006.13047 \[gr-qc\]](#).
- [51] C.-K. Qiao and M. Zhou, *JCAP* **12**, 005 (2023), [arXiv:2212.13311 \[gr-qc\]](#).
- [52] E. Gallo and T. Mädler, *Eur. Phys. J. C* **85**, 299 (2025), [arXiv:2412.10328 \[gr-qc\]](#).
- [53] A. Kumar, A. Sood, S. G. Ghosh, and A. Beesham, *Particles* **7**, 1017 (2024).
- [54] A. Bhattacharyya, W. Chemissany, S. S. Haque, J. Murugan, and B. Yan, *SciPost Phys. Core* **4**, 002 (2021), [arXiv:2007.01232 \[hep-th\]](#).
- [55] A. Anand, S. Noori Gashti, and A. Singh, *Phys. Dark Univ.* **49**, 101994 (2025), [arXiv:2506.23736 \[gr-qc\]](#).
- [56] A. Singh, A. Modak, and B. Panda, (2025), [arXiv:2507.02716 \[gr-qc\]](#).
- [57] R. Banerjee and D. Roychowdhury, *Phys. Rev. D* **85**, 104043 (2012).
- [58] R. Banerjee and D. Roychowdhury, *Phys. Rev. D* **85**, 044040 (2012).